J MATER SCI 41 (2006) 653–660

The effect of twinning interactions up to the seventh generation on the evolution of microstructure

VALERIE RANDLE
Materials Research Centre, School of Engineering, University of Wales Swansea, Swansea, UK

The investigation reported here extends the conventional approach to the study of the interface network, by consideration of $\Sigma 3^n$ values up to $n = 7$ in alpha-brass. All 24 crystallographically-related solutions for each $\Sigma 3^n$ misorientation are included. The study has shown that multiple annealing twinning does not result in aggregation of higher $\Sigma 3^n$ values and concomitant reduction in Σ3s. When a 5° deviation from the exact reference misorientation was used, 20% and 27% of the interface length was Σ729 and Σ2187 respectively. This is a consequence of the increasing number of $\Sigma 3^n$ variants as n increases. Interactions of $\Sigma 3^n$, often $\Sigma 3 + \Sigma 3^n \leftrightarrow \Sigma 3^{n+1}$, were observed frequently in the microstructure. The prevalence of boundaries near to high order $\Sigma 3^n$ attests their importance in the evolution of microstructure. Analysis of all 24 equivalent solutions for $\Sigma 3^n$ boundaries has shown that approximately half of these are misoriented on ⟨110⟩, compared to less than one-third on ⟨111⟩. The promulgation of $\Sigma 3^n$ boundaries via multiple twinning interaction events promotes and increases the proportion of ⟨110⟩ tilt boundaries, and to a lesser extent ⟨111⟩ boundaries. These misorientations have been shown to be associated with low-index boundary planes, and therefore multiple twinning is instrumental in promoting these 'special' planes.

1. Introduction

Both the crystallography and the properties of the interface network in polycrystalline materials are influenced by the presence of annealing twins, especially in low stacking-fault energy metals and alloys where twinning is prolific. In coincidence site lattice (CSL) notation twins are one type of $\Sigma 3$ boundary, where Σ refers to the reciprocal density of coinciding sites. A prerequisite for most 'grain boundary engineered', GBE, materials is that a high proportion of the total interface area, typically >50%, is $\Sigma 3$, which leads to improved properties in terms of overall resistance to intergranular degradation [1]. The mechanisms of GBE in terms of how Σ3s affect the grain boundary network characteristics are not yet completely understood. It is therefore of interest to study the role that $\Sigma 3$ and higher order $\Sigma 3^n$ play in evolution of the interface network.

During grain growth, interfaces impinge and new triple junctions (i.e. grain edges) are formed. The crystallographic constraints at a triple junction give rise to a 'sigma combination rule', which states that

$$\Sigma_3 = \Sigma_1 \Sigma_2 / \alpha \tag{1}$$

where Σ_1, Σ_2 and Σ_3 refer to the Σ values of the component boundaries in the junction, α is the greatest common divisor of the integer matrix $(\Sigma_1 R_1 \cdot \Sigma_2 R_2)$, where R_1 and R_2 are the corresponding misorientation matrices [2]. Prolific annealing twinning accompanied by grain boundary migration leads to many interactions whereby $\Sigma 3^n$ boundaries are generated at triple junctions, according to equation 1. Triple junctions containing $\Sigma 3$ always have $\alpha = 1$. For this case one of the Σs in the junction is simply a product of the other two, e.g. a junction could comprise an encounter between a $\Sigma 3$ and a $\Sigma 9$ to form a new $\Sigma 27$. This can be written as $\Sigma 3^1 + \Sigma 3^2 \rightarrow \Sigma 3^3$. Alternatively, according to equation 1 an encounter between a $\Sigma 9$ and a $\Sigma 3$ could give a $\Sigma 3$ boundary rather than a $\Sigma 27$, i.e. $\Sigma 3^1 + \Sigma 3^2 \rightarrow \Sigma 3^1$. Interactions of the latter type are important in the development of GBE materials because they supplement the $\Sigma 3$ population, and Σ3s

0022-2461
DOI: 10.1007/s10853-006-6481-3

generally have 'special' properties. This is known as the 'Σ3regeneration model' [3].

In a GBE material, because Σ3s are so prolific many triple junctions will inevitably be composed of $\Sigma 3^n$ boundaries. The interaction of $\Sigma 3^n$ boundaries is hence central to the development of the interface network in highly twinned materials. Only a few studies of multiple twinning have sought to investigate the role that $\Sigma 3^n$, $n>3$, boundaries play in the evolution of the microstructure [4, 5]. Instead, experimental studies on GBE metals and alloys usually only record $\Sigma 3^n$ values up to $n = 3$, i.e. Σ27, and ignore higher values of n. This has been largely because the focus of Σ characterisation was only to link low-Σ boundaries with properties. However it is now contended that, apart from Σ3, the CSL is an unreliable predictor of 'special' properties and its main role is as a categorisation tool [6]. The investigation reported here extends the conventional approach to the study of the interface network by inclusion of $\Sigma 3^n$ values up to $n = 7$.

Another feature of most GBE interface categorisation studies is that they consider only 'disorientation', i.e. that misorientation solution (of the 24 equivalent ones) which contains the lowest angle. This approach overlooks certain important features of the interface network, for example that not all low-index misorientation axes are revealed by the disorientation solution. The present investigation, therefore, also focuses on the inclusion of all 24 crystallographically-related solutions for each $\Sigma 3^n$ misorientation.

2. Experimental

A specimen of alpha-brass (70% Cu, 30% Zn) underwent thermomechanical processing by five iterations of 25% uniaxial strain followed by annealing in air for 300s at 665°C. This processing produced a 'grain boundary engineered' microstructure dominated by a high proportion of Σ3 and $\Sigma 3^n$ interfaces. Full details of the processing, specimen preparation and effect on properties have been published elsewhere [7]. Many high resolution electron back-scatter diffraction (EBSD) orientation maps of the specimen were obtained using HKL Channel 5 software interfaced to a Philips XL30 scanning electron microscope operated at an accelerating voltage of 20 kV. Maps were obtained by beam scanning followed by montaging contiguous regions. A step size of 2 μm was used for mapping. Approximately 20,000 grains comprised the total dataset. Proportions of $\Sigma 3^n$ boundaries up to $n = 7$ were obtained using Channel 5 software which had been specially adapted by the author for this purpose. All 24 crystallographically-related solutions were calculated using an in-house algorithm.

3. Results and discussion

Table I lists the disorientation solutions (axis and angle) for all $\Sigma 3^7$ boundaries. The axis is given in the form of Miller indices. The number of variants increases as Σ increases, giving the following number of solutions:

$$\Sigma 9(\Sigma 3^2) - 1$$
$$\Sigma 27(\Sigma 3^3) - 2$$
$$\Sigma 81(\Sigma 3^4) - 4$$
$$\Sigma 243(\Sigma 3^5) - 9$$
$$\Sigma 729(\Sigma 3^6) - 19$$
$$\Sigma 187(\Sigma 3^7) - 33$$

The proportions of $\Sigma 3^7$ boundaries in a region of specimen comprising nearly 1500 grains was calculated according to three tolerances: the Brandon criterion [8], 2° tolerance and, as in [5], 5° tolerance. Because the Brandon criterion has a $\Sigma^{-\frac{1}{2}}$ dependency, very large Σ values have small tolerances, i.e. only 0.32° for Σ2187 and 0.56° for Σ729. This is at the error limit for EBSD misorientation measurement, which is usually considered to be 0.5°. Furthermore in order to track the evolution of boundary types in the microstructure according to the Σ combination rule, it is more appropriate to exercise a larger acceptance criterion because frequently $\Sigma 3^n$ boundaries (except most twins) are displaced from the reference misorientation. For example, for the data recorded here, less than half of Σ9 boundaries are within 1° of the reference. It can easily be envisaged that this deviation from the reference structure will accumulate with increasing $\Sigma 3^n$, because $\Sigma 3^n$ with higher n values are the result of interactions between other $\Sigma 3^n$ values. Some examples of triple junction interactions from the present data set are shown below.

Fig. 1 shows the proportions of $\Sigma 3^n$ as a fraction of the total interface length according to the Brandon maximum, 2° tolerance and 5° tolerance. More than half of the interface length is Σ3, i.e. 57.7% according to the Brandon criterion, which designates Σ3s as within 8.7° of the reference misorientation. Whereas this is a large tolerance, in fact practically all of the Σ3 length is within 2° of the reference structure, as shown in Fig. 1. For Σ9, the Brandon tolerance is 5°. Similarly to the case for Σ3s, most of the Σ9 length falls in the 2° category. For Σ27 the Brandon criterion is 2.9°, and the proportion of Σ27s increases slightly from 1.9% to 2.3% when the acceptance angle is widened to 5°. As pointed out in the Introduction, frequently only $\Sigma 3^n$ up to Σ27 are reported when grain boundary statistics are compiled. The trend found here, where Σ9 and Σ27 are very small compared to Σ3, has been observed before in a GBE alloy and is indicative of the 'Σ3 regeneration model' whereby multiple twinning does not aggregate the proportion of Σ9 and Σ27, but rather these boundaries dissociate to produce more Σ3s.

TABLE I Disorientation solution and deviation from nearest ⟨110⟩ and ⟨111⟩ axes (from all 24 misorientation solutions) for $\Sigma 3^n$, $n \leq 7$

Σ	Disorientation axis (in Miller indices)	Disorientation angle (in degrees)	Deviation angle from nearest ⟨110⟩ axis	Deviation angle from nearest ⟨111⟩ axis
3	111	60	0	0
9	110	38.94	0	11.4
27a	110	31.58	0	9.4
27b	210	35.42	5.8	11.5
81a	411	38.94	11.1	11.4
81b	322	54.53	3.7	5.2
81c	531	38.38	5.8	9.3
81d	443	60.41	0	3.7
243a	955	43.08	10.5	6.1
243b	761	49.75	3.5	10.9
243c	311	12.21	3.2	3.3
243d	542	35.43	5.8	5.8
243e	655	49.75	6.2	2.1
243f	971	43.08	3.4	11.1
243g	411	31.59	8.9	9.5
243h	706 706 64	60.00	2.1	5.6
243i	110	7.36	0	2.4
729a	787	38.94	11.1	1.3
729b	951	22.09	3.2	6.4
729c	803 519 292	54.15	6.9	9.5
729d	758 416 552	59	3.3	6.7
729e	737	22.09	3.2	3.7
729f	483	28.61	6.4	5.9
729g	143	44.38	5.6	9.3
729h	786 524 328	47.13	9.3	7.5
729i	958 56 282	49.7	9.5	13.1
729j	661 485 573	49.7	6.6	3.0
729k	588	54.53	4.2	5.2
729l	314 864 393	38.94	9.2	8.2
729m	292	28.61	8.2	9.1
729n	231	11.25	1.9	2.3
729o	720	31.28	7.7	11.5
729p	633 518 575	54.15	3.8	2.1
729q	45 749 661	49.7	2.0	10.5
729r	461	31.28	3.8	7.3
729s	677 521 521	60.41	0	3.7
2187a	844 379 379	43.08	11.0	8.1
2187b	816 381 435	46.3	9.1	7.7
2187c	867	21.27	5.3	1.3
2187d	611 36 791	49.75	3.5	10.6
2187e	272 653 707	46.3	6.7	7.7
2187f	283 629 724	57.44	4.5	9.1
2187g	54 11 998	26.72	9.0	11.3
2187h	82 983 163	21.27	6.3	8.1
2187i	478 869 131	40.74	6.5	10.7
2187j	600 180 800	29.2	3.4	6.7
2187k	755	12.21	3.2	1.1
2187l	442 694 568	39.6	9.2	3.5
2187m	538 794 282	49.32	8.8	8.8
2187n	795 497 348	35.43	7.4	5.8
2187o	409 661 629	57.44	2.4	5.4
2187p	66 66 36	29.2	5.4	3.7
2187q	302 719 626	54.9	5.6	8.2
2187r	298	21.27	1.9	5
2187s	877	31.59	8.9	1
2187t	369 469 803	53.72	5.3	8.4
2187u	156 822 548	45.46	6.0	10.7
2187v	400 711 578	57.5	4.2	6.1
2187w	43 999 3	40.74	14.1	16.9
2187x	925 0 380	46.3	9.4	13.7
2187y	535 703 468	53.72	4.3	4.5
2187z	315 63 947	39.6	9.2	13
2187aa	417 686 596	60.95	2.4	5.6
2187bb	114	7.36	2.0	2.4
2187cc	694 189 694	39.6	3.9	8.2
2187dd	599 151 786	35.81	3.7	8.4
2187ee	994 50 100	35.43	11.5	13.9
2187ff	509 694 509	26.72	7.1	2.1
2187gg	110	46.3	0	12.1

In the present data where higher $\Sigma 3^n$ values are recorded, those with $n>3$ similarly are present in small proportions (where the acceptance criterion is the Brandon criterion or 2°) showing further evidence that multiple twinning does not result in aggregation of higher $\Sigma 3^n$ values.

For $\Sigma 3^n$ ($n>3$) the Brandon criterion is less than 2°. It can be seen in Fig. 1 that, whereas the proportions of $\Sigma 3^n$ with $n>3$ are insignificant according to the Brandon criterion and very small with the 2° acceptance criterion, increasing the acceptance angle to 5° has a dramatic effect on the proportions recorded. For example for the highest Σ values, Σ729 and Σ2187, the proportion increases from .06% and .01% respectively with the Brandon criterion to 20% and 27% respectively with a 5° tolerance. This is a consequence of the increasing number of misorientation variants as n increases: there are 19 variants of Σ729 and 33 variants of Σ2187. It can be noted that the statistics for the 5° tolerance total more than 100%. This indicates that when the acceptance angle is widened, there is inevitably some overlap between classes, and so some boundaries are counted more than once. For example, Σ729p and Σ729s are 5.6° and 5.9° respectively from Σ3 (see Table I). Even so, use of the 5° criterion is justified in terms of tracking interactions between boundaries, as demonstrated below, and moreover the prevalence of boundaries near to high order $\Sigma 3^n$ attests their importance in the evolution of microstructure.

Proportions of Σ types can be compiled according to a length fraction or a number fraction. Fig. 2 shows that the number fraction is the larger statistic, except for Σ3 where the length fraction is very much larger than the number fraction. This is due to the morphology of annealing twins, namely that they often extend across the entire width of a grain and often occur in pairs or multiples. Using the 2° criterion, 72% of the interface length is $\Sigma 3^n$ and 61% of the number of interfaces is $\Sigma 3^n$.

Fig. 3 shows the distribution of $\Sigma 3^7$ boundaries in one region of the brass specimen. $\Sigma 3^n$ boundaries up to $n = 7$ (2° tolerance) are depicted as grey lines and the remaining random boundaries are wide black lines. It can be seen that the $\Sigma 3^n$ interfaces greatly fragment the grain boundary network.

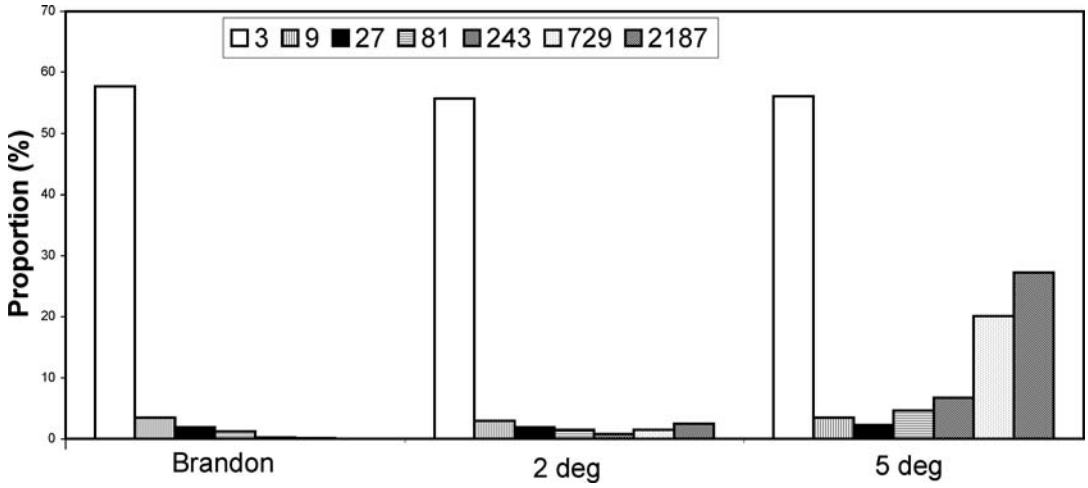

Figure 1 Graph of $\Sigma 3^n$ (n=1 to 7) proportions in GBE brass specimens, according to the Brandon criterion, 2° tolerance and 5° tolerance.

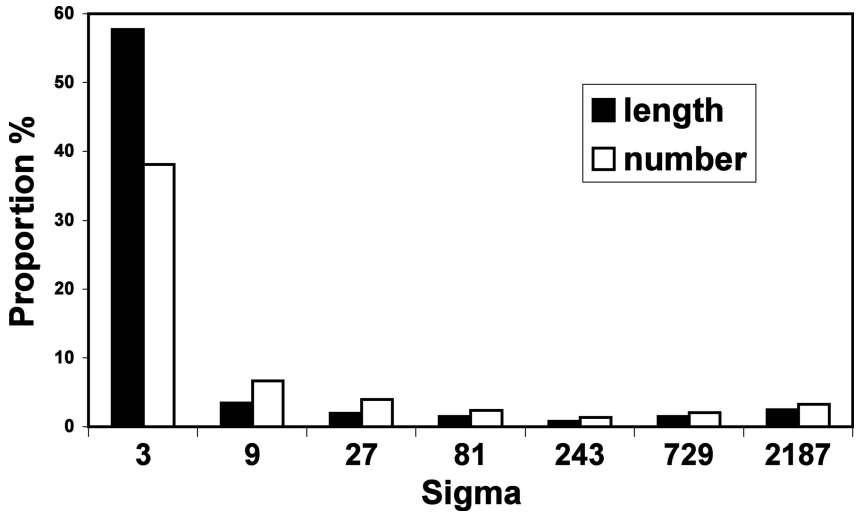

Figure 2 Graph of $\Sigma 3^n$ (n=1 to 7) proportions in GBE brass specimens (2° tolerance) according to both length fraction and number fraction.

Figs 4a and b show enlarged sections taken from Fig. 3. In Fig. 4 each boundary is labelled with its n value or labelled 'R' if the boundary is random. Boundaries are labelled using the 5° tolerance in order to portray boundary interactions. In many cases at least one $\Sigma 3$ is a component of triple junctions, because more than half of the interface length is $\Sigma 3$. Such junctions typically comprise $\Sigma 3$, $\Sigma 3^n$ and $\Sigma 3^{n+1}$, and there are many examples in Fig. 3 and Fig. 4 of this junction configuration. The 'classic' configurations of $\Sigma 3$-$\Sigma 3$-$\Sigma 9$ and $\Sigma 3$-$\Sigma 9$-$\Sigma 27$ (n values 1-1-2 and 1-2-3 respectively) are observed frequently. Other interactions which obey the addition rule in equation 1 but incorporate higher Σ values are also observed, for example $\Sigma 3$-$\Sigma 243$-$\Sigma 729$ and $\Sigma 3$-$\Sigma 27$-$\Sigma 81$ (n values 1-5-6 and 1-3-4 respectively) feature in Fig. 4. In both these triple junctions the $\Sigma 3$ boundaries were within 1° of the reference structure in both triple junctions. Details of the disorientations of the other boundaries in the junctions are:

55.4°/726, 107, 679, 4.4° from $\Sigma 243$h

28.2°/864, 435, 253, 1.5° from $\Sigma 729$f

41.2°/822, 517, 238, 3.2° from $\Sigma 81$c

29.7°/52, 726, 685, 1.4° from $\Sigma 27$a

Clearly each of these boundaries violates the Brandon criterion, but use of the 5° criterion permits the observation of $\Sigma 3^n$ interactions according to equation 1. On the other hand use of the 5° criterion sometimes means that the addition rule is violated. This is observed especially where $\Sigma 2187$ is involved. For example a junction designated $\Sigma 3$-$\Sigma 27$-$\Sigma 2187$ (n values 1-3-7), which does not conform to the addition rule, features in Fig. 4. In summary, the data in Fig. 4 demonstrates the

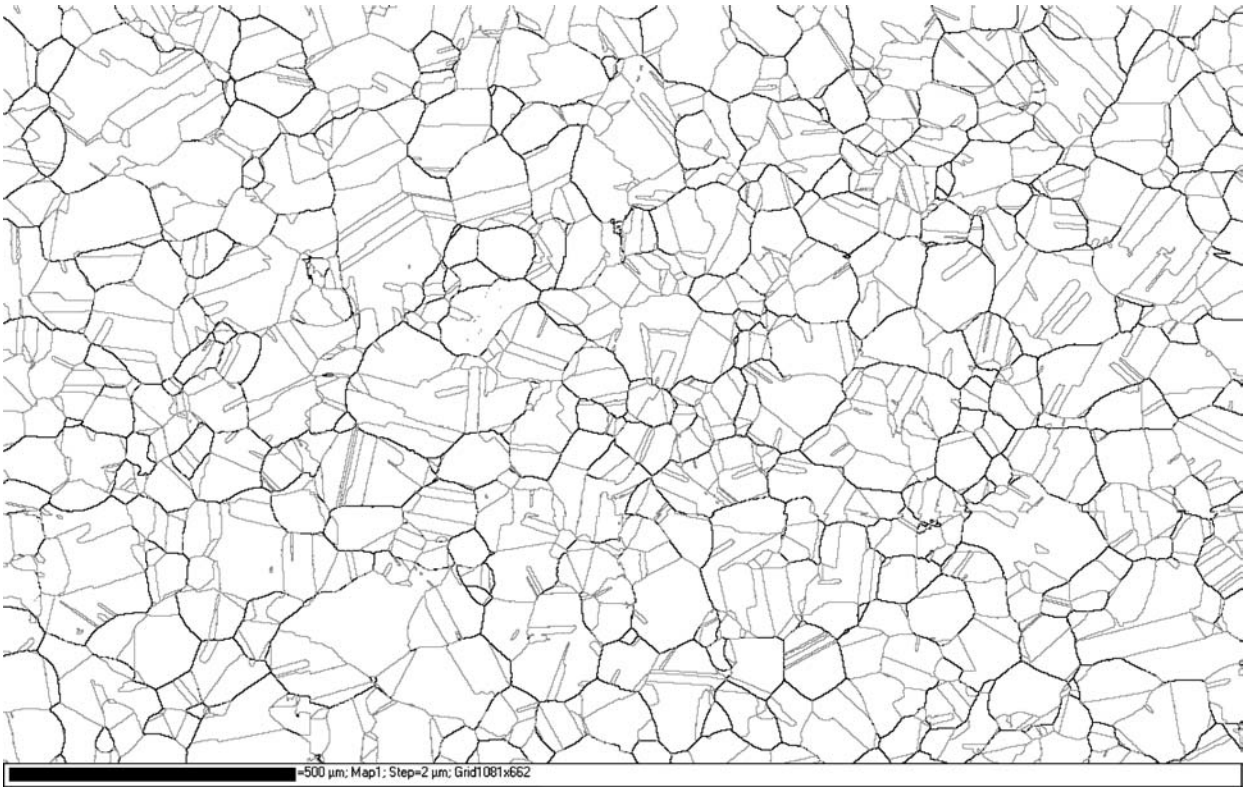

Figure 3 Distribution of $\Sigma 3^7$ boundaries in one region of the brass specimen. $\Sigma 3^n$ boundaries up to $n = 7$ (2° tolerance) are depicted as grey lines and the remaining random boundaries are wide black lines.

pervasion of $\Sigma 3^n$ interactions in the microstructure when there is a high proportion of $\Sigma 3$s present.

Interactions at triple junctions can usually be described by three rotations about a common axis, where the sum of the three misorientation angles totals 360°. For example

$$70.53^\circ/\langle 110\rangle + 141.06^\circ/\langle 110\rangle \leftrightarrow 211.59^\circ/\langle 110\rangle \quad (2a)$$

$$\Sigma 3 + \Sigma 9 \leftrightarrow \Sigma 27a \quad (2b)$$

The misorientations in equation 2a are not the disorientation solutions, but rather one of the other equivalent solutions for the misorientation. As an illustration Table II lists misorientation interactions between $\Sigma 3$ boundaries and other $\Sigma 3^n$ on the ⟨110⟩ axis up to $\Sigma 3 + \Sigma 3^8 \leftrightarrow \Sigma 3^9$. For each $\Sigma 3^{n+1}$ misorientation the equivalent disorientation is also listed. For some cases the disorientation is also on ⟨110⟩ whereas in other cases, i.e. for $\Sigma 81$, $\Sigma 729$ and $\Sigma 19683$, the disorientation axis is not ⟨110⟩. It is clear that inspection of the disorientation alone does not predict that one of the other equivalent solutions is on ⟨110⟩.

Previous work to measure the distribution of both misorientations and planes in GBE brass has shown that ⟨110⟩ and ⟨111⟩ misorientation axes are significant because a high proportion of interface, even when coherent twins are excluded, is composed of ⟨110⟩ asymmetric tilt and ⟨111⟩ twist boundaries [9]. This finding supplements the more general conclusion, based on measurement of boundary planes in a variety of systems, that there is an inverse relationship between the frequency with which boundaries occur in the population and their energy. Therefore it can be assumed that boundary types with high populations are also low energy boundaries [10]. This assumption is supported by the results of calculations which have shown that asymmetric boundaries may have low energies when bounded by low-index planes [11] and that ⟨110⟩ tilts in particular lie in an energy valley [12].

In the present work, it is of value to ascertain if the $\Sigma 3^n$ boundaries have misorientation axes which are close to either ⟨110⟩ or ⟨111⟩, because boundaries with these misorientation axes in this specimen are associated with tilt and twist boundaries respectively, as described above. Table I therefore also includes the deviation angle from nearest ⟨110⟩ axis and the nearest ⟨111⟩ axis out of the entire 24 equivalent solutions.

It transpires that nearly half (32 out of 69) of the misorientations listed in Table I are misoriented within 5° of a ⟨110⟩ axis. On the other hand less than one-third (19 out of 69) of misorientations listed in Table I are misoriented within 5° of a ⟨111⟩ axis. In consequence the average deviation of the misorientation axes in Table I from ⟨111⟩ and ⟨110⟩ is 7.2° and 5.5° respectively. Seven misorientations are exactly on a ⟨110⟩ axis, and these are listed in

TABLE II Interactions between Σ3 boundaries and other $\Sigma 3^n$ on ⟨110⟩

Misorientation angle for Σ3	Misorientation angle for $\Sigma 3^n$	$\Sigma 3^n$ value	Misorientation angle for $\Sigma 3^{n+1}$	$\Sigma 3^{n+1}$ value	Equivalent disorientation for $\Sigma 3^{n+1}$
70.53	70.53	3	141.06	9	38.94/110
70.53	141.06	9	211.59	27	31.59/110
70.53	211.59	27	282.11	81	60.40/443
70.53	282.11	81	352.65	243	7.36/110
70.53	352.65	243	63.18	729	60.42/13, 10, 10
70.53	63.18	729	133.71	2187	46.30/110
70.53	133.71	2187	204.24	6561	24.23/110
70.53	204.24	6561	274.77	19683	61.63/661, 661, 355

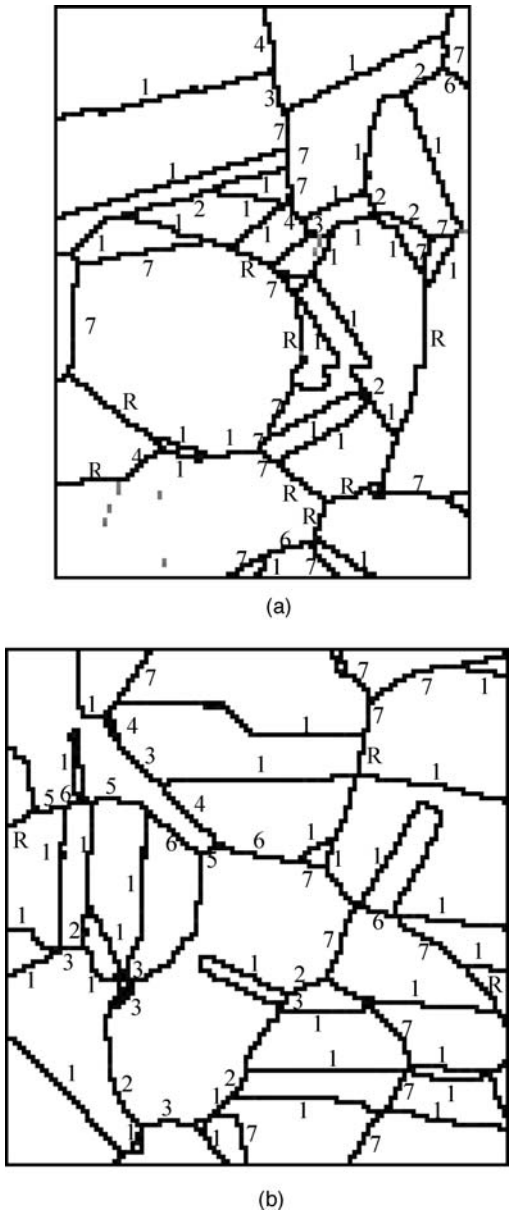

Figure 4 Two sections of Fig. 3 with all boundaries in black. Boundaries are labelled according to *n* values or *R* for random boundary.

Table II. By contrast the only misorientation axis exactly on ⟨111⟩ is Σ3, which is a special case because it also has a misorientation solution on ⟨110⟩. Apart from Σ3, the minimum deviation from a ⟨111⟩ axis is 1°. The maximum deviation from ⟨111⟩ and ⟨110⟩ is 16.2° and 14.1° respectively. These deviations refer to the same misorientation (Σ2187w). The large deviation is because the disorientation axis is 999, 43, 0, i.e. very close to 100. Similarly, the second largest deviation from ⟨111⟩ and ⟨110⟩ is 13.9° and 11.5° respectively (Σ2187ee), which also corresponds to a disorientation axis close to 100.

Features of the ⟨110⟩ and ⟨111⟩ misorientation deviation distribution are illustrated on Fig. 5. Fig. 5a shows the deviation distribution of ⟨110⟩ (dev_{110}) versus that of ⟨111⟩ (dev_{111}). The linear regression of dev_{111} is included as a straight solid line. It can be seen that there is a correlation between the values, except for the cases where $dev_{110} = 0$. There is a discontinuity in the values between zero deviation from ⟨110⟩ and the remainder of the values, wherein the distribution is continuous. This is more clearly illustrated on Fig. 5b, where the deviation from ⟨110⟩ values have been arranged in ascending order.

The most important finding from examination of the dev_{110} and dev_{111} distributions is that approximately half of the $\Sigma 3^n$ values are misoriented on ⟨110⟩. Because previous work on the same GBE specimens had shown that ⟨110⟩ misorientations are asymmetric tilt boundaries, it is a significant result that the '24-solutions' analysis has shown that promulgation of $\Sigma 3^n$ boundaries via multiple twinning interaction events promotes and increases the proportion of ⟨110⟩ boundaries. ⟨110⟩ tilt boundaries can be asymmetric types having one {111} plane at the boundary, where the 'opposite' boundary plane is dictated by the misorientation. ⟨111⟩ misorientation axes (apart from Σ3) feature less in the microstructure than ⟨110⟩ axes, which indicates that there is less chance to form ⟨111⟩ twist boundaries than ⟨110⟩ tilt boundaries. This concurs with previous data which showed in these specimens that the density of ⟨111⟩ twist boundaries was far less than that of ⟨110⟩ tilt boundaries, whereas overall in the specimens the most prevalent boundary plane was {111}(excluding twins) [9].

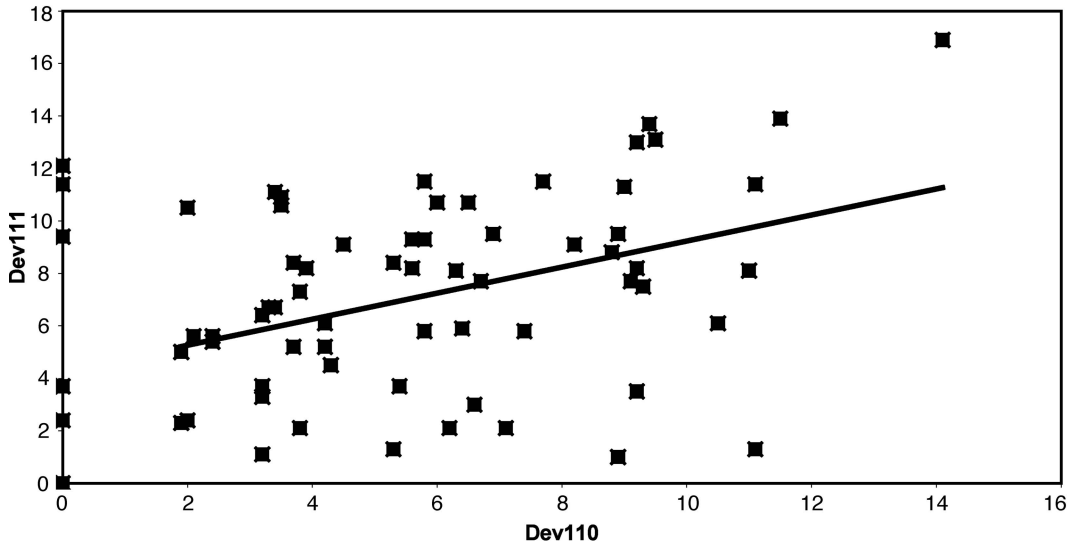

(a)

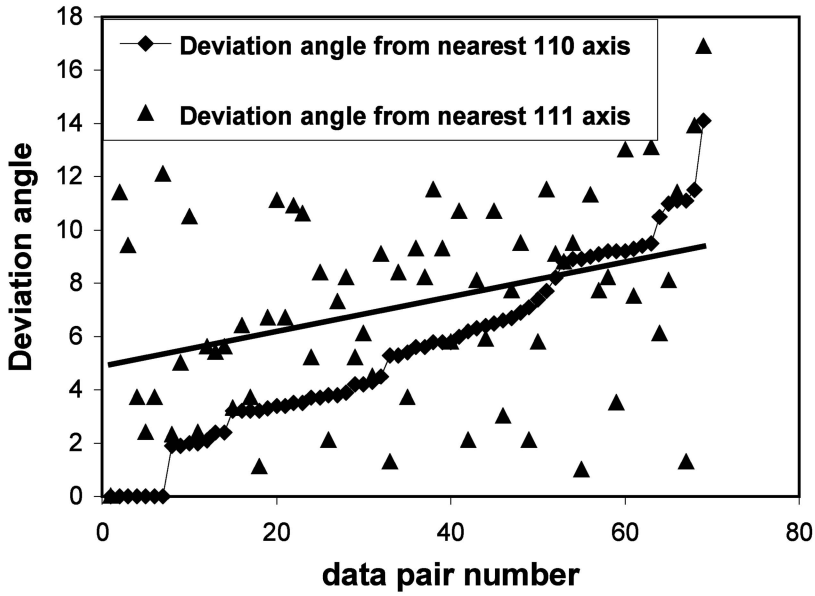

(b)

Figure 5 Graph of (a) the misorientation solution having the minimum deviation from 110 (dev_{110}) versus the misorientation solution having the minimum deviation from 111 (dev_{111}). (b) as in (a), with dev_{110} in ascending order. Lines joining dev_{110} are only to guide the eye. The linear regression of dev_{111} is included as a straight solid line.

Finally, the analysis presented here has shown how the evolution of a misorientation distribution is influenced by $\Sigma 3^n$ interactions. It must be stressed that the evolution in terms of Σ value is geometrical and crystallographic only, and does not infer a link between Σ value and properties. In fact, only $\Sigma 3$ boundaries are know to be associated with superior mechanical and corrosion properties [1, 13]. The mechanism of GBE is thought to be associated with the fragmentation of the grain boundary network by $\Sigma 3$s and, according to recent evidence, by the presence of low-index boundary planes in the remaining boundary network, i.e. not including $\Sigma 3$s. The results presented here give further indirect support to this contention.

4. Conclusions

$\Sigma 3$ ($n \leq 7$) misorientations have been analysed in grain boundary engineered alpha-brass. The main conclusions from the study are

1. Multiple twinning does not result in aggregation of higher $\Sigma 3^n$ and a concomitant reduction in $\Sigma 3$.

2. When a 5° deviation from the exact reference misorientation is used, 20% and 27% of the interface length is $\Sigma 729$ and $\Sigma 2187$ respectively, compared to 0.06% and 0.01% respectively when the Brandon criterion is applied. This is a consequence of the increasing number of $\Sigma 3^n$ variants as n increases. The prevalence of boundaries near to high order $\Sigma 3^n$ attests their importance in the evolution of microstructure.

3. Interactions of $\Sigma 3^n$, often $\Sigma 3 + \Sigma 3^n \leftrightarrow \Sigma 3^{n+1}$, are observed frequently in the microstructure.

4. The convention of reporting only the disorientation (of the 24 equivalent solutions) is not the most appropriate means of tracking interactions at triple junctions.

5. Analysis of all 24 equivalent solutions for $\Sigma 3^n$ boundaries has shown that approximately half of these are misoriented on ⟨110⟩, compared to less than one-third on ⟨111⟩. The promulgation of $\Sigma 3^n$ boundaries via multiple twinning interaction events promotes and increases the proportion of ⟨110⟩ boundaries, and to a lesser extent ⟨111⟩ boundaries. These misorientations have been shown to be associated with low-index boundary planes, and therefore multiple twinning is instrumental in promoting these 'special' planes.

References

1. V. RANDLE, *Acta Mater.* **52** (2004) 4067.
2. V. Y. GERTSMAN and C. H. HENAGER, *Inter. Sci.* **11** (2003) 403.
3. V. RANDLE, *Acta Mater.* **47** (1999) 4187.
4. G. GOTTSTEIN, *Acta Metall.* **32** (1984) 1117.
5. V. Y. GERTSMAN, in Science and Technology of Interfaces, edited by S. Ankem, C. S. Pande, I. Ovid'ko and S. Ranganathan (TMS, 2002) p. 387.
6. V. RANDLE, *Scripta Mater* (in press).
7. V. RANDLE and H. M. DAVIES, *Mater. Trans. A* **33** (2002) 1853.
8. D. G. BRANDON, *Acta Metall.* **14** (1966) 1479.
9. C. KIM, Y. HU, G. ROHRER and V. RANDLE, *Scripta Mater.* **52** (2005) 633.
10. D. M. SAYLOR, B. S. EL-DASHER, A. D. ROLLETT and G. S. ROHRER, *Acta Mater.* **52** (2004) 3649.
11. K. L. MERKLE and D. WOLF, *Philos. Mag. A* **65** (1992) 513.
12. U. WOLF, F. ERNST, T. MUSCHIK, M. W. FINNIS and H. F. FISCHMEISTER, *ibid.* **66** (1992) 991.
13. V. Y. GERTSMAN and S. M. BRUEMMER, *Acta Metall. Mater.* **42** (1994) 1785.